Shale Graptolite Thermometers and Its Indication of Organic Matter Maturity in the Three Gorges Area

Jiaming Shen

Room 1-101, 330 Minzu Avenue, Wuhan, Hubei Province, 430074, China
Author: Jiaming, Shen, Email: shenjiaming2025@126.com

Abstract

Organic matter maturity evaluation is an important research content in shale gas exploration. A comprehensive analysis combining various types of indicators may be a way to obtain relatively accurate organic matter maturity results. The Wangjiawan Upper Ordovician Wufeng - Longmaxi Formation shale section was selected as research objects in the Three Gorges area. 16 samples of various graptolite fossils, 5 Longmaxi Formation black shale samples, 2 Hernanterbe fossil samples, and 2 trilobite fossil samples were collected for experiments. Graptolites epidermal reflectance, bitumen reflectance and Raman spectroscopy reflectance were used to calculate the organic matter maturity, and then to establish the interrelationships between them. The equivalent vitrinite reflectance converted from solid bitumen reflectance is 1.098-1.110%, the shale maturity revealed by graptolite reflectance is 1.245-1.253%, and the average organic matter maturity obtained from calculations based on organic matter Raman spectroscopy is 0.7415~0.9663%. The correlation between solid bitumen reflectance and graptolite epidermis reflectance was 0.7663, between solid bitumen reflectance and Raman spectroscopy reflectance is 0.9748, and between graptolite epidermis reflectance and Raman spectroscopy reflectance is 0.6203. All are greater than 0.6, and these three methods can be used to characterize the organic matter maturity. A relationship between graptolite reflectance and paleotemperature has been established. Graptolite reflectance can serve as a temperature indicator for the maturity of shale organic matter, and it is the best and relatively more accurate indicator compared to solid bitumen reflectance and Raman spectroscopy reflectance.

Keywords

Introduction

The widely distributed Upper Ordovician Wufeng - Lower Silurian Longmaxi Formation marine black shale are high-quality hydrocarbon source rocks (Jin et al., 2016; Wang et al., 2019) in the Yangtze Block, and also a set of key formations for the present shale gas exploration and development in China (Guo et al., 2014). Black shale organic matter maturity determines the stage of hydrocarbon evolution, and also closely related to shale pore structure and gas content (Hao et al., 2013; Mastalerz et al., 2013; Luo et la., 2017, 2020). Therefore, organic matter maturity evaluation has been an important research content in shale gas exploration.

Citation: Jiaming Shen. (2024) Shale Graptolite Thermometers and Its Indication of Organic Matter Maturity in the Three Gorges Area. Researchers 1(44): e20240919

Received on August 15, 2024; Accepted on August 22, 2024; Published on September 19, 2024

Vitrinite reflectance is currently the only internationally comparable indicator of maturity (Tissot and Ilte, 1984). However, vitrinites are derived from lignin in higher plants after the Silurian, so vitrinite reflectance (VRo), the most commonly used indicator of organic matter maturity cannot be used in the Lower Paleozoic, which creates great difficulties in accurately evaluating the black shale thermal maturity of the Wufeng - Longmaxi Formation (Qiu et al., 2012; Luo et al., 2019). To address this problem, in Lower Paleozoic shales lacking vitrinite bodies, the maturity evaluation is usually performed by applying bitumen reflectance (VRb) as the equivalent vitrinite reflectance through converting formulae. However, bitumen exists from multiple sources and coexists in multiple stages (Peters et al., 2013; Bertrand, 1990, 1993), the relationship between bitumen reflectance and vitrinite reflectance is complex in different basins, and bitumen existed in different lithologies varies (Bertrand, 1990, 1993), and the formulae for converting the different maturity stages may be different (Wang et al., 2019). As a result, there have also been some controversies about bitumen as a maturity parameter, and Hackley and Cardott (2016) also noted that existing empirical conversion formulas should be used with caution.

In recent years, some scholars began to pay attention to the graptolites epidermal reflectance, e.g., Yang Yunfeng (2016) compared the difference between the bitumen reflectance and the graptolites reflectance of the Silurian Longmaxi Formation shales in southeastern Sichuan basin and pointed out that the Longmaxi Formation shale are the high – over maturity stage. Luo Qingyong et al. (2017) investigated the graptolites' organic matter optical characteristics and determined thermal maturity of the Wufeng - Longmaxi Formation shale in southeast Chongqing area through the maximum reflectance value of graptolites. Wang et al. (2019) explored maturity distribution characteristics of the Wufeng - Longmaxi Formation shale by using the stochastic reflectance of graptolites epithermal bodies on the vertical laminar sections in the Sichuan Basin and its periphery area. Luo Qingyong et al. (2020) conducted a systematic review of the current research status on graptolites as geothermometers. And more and more studies have been conducted on the application of the reflectance of graptolites' epidermal bodies to determine shale organic matter maturity. However, there are no clear and unified understandings of the conversion relationship between graptolites' epidermal reflectance and equivalent vitrinite reflectance, and it is difficult to accurately convert graptolites' epidermal reflectance to equivalent vitrinite reflectance with the existing formulas (Meng et al., 2022). There are also more scholars evaluating matter maturity based on Raman spectroscopy (Guede et al., 2010; Liu et al. 2013; Wilkins et al. 2014, 2015; Wang and Li, 2016; Wang et al. 2021). Liu et al. (2013) and Wilkins et al. (2014, 2015) established two quantitative characterization formulas using solid organic matter Raman spectroscopic parameters to evaluate the organic matter maturity degree. However, the applicability of Raman spectroscopic parameters is correlated with thermal maturity stage of the samples (Meng et al., 2022), and low-maturity samples may have fluorescence interferences that make the experimental data more dispersed (Quirico, 2005; Henry, 2018), whereas the precision of Raman spectroscopic parameters of highly-over mature samples is very high (Liu et al., 2013).

In summary, in order to evaluate the organic-rich marine black shale maturity of the Upper Ordovician Wufeng - Lower Silurian Longmaxi

Formation, a comprehensive analysis combining various types of indicators may be a way to obtain relatively accurate results. In this work, the Wangjiawan Upper Ordovician Wufeng - Longmaxi Formation shale section will be selected as research objects in the Three Gorges area. To study the special optical properties of graptolites epidermal body, systematically analyze the optical reflectivity characteristics of shale organic matter micro-components, bitumen reflectance and Raman spectroscopy reflectance, to establish the interrelationships between them, and to explore the method of equivalent vitrinite reflectance conversion, so as to more objectively, accurately, and comprehensively determine the thermal maturity degree of the Wufeng - Longmaxi Formation shale of the Wangjiawan section in Three Gorges area. This study would provide the important information about organic matter maturity for exploration and evaluation of shale gas.

Literature review

What is Graptolite?

Graptolite sounds “Bishi” in Chinese which will make us wonder if the name has anything to do with pens. In fact, the naming of graptolite does have something to do with pens. Graptolite refers to the fossils of graptolites, due to its state of preservation, it is flattened into a carbonaceous film, and its appearance resembles the traces of pencil writing or scribbling on the rock surface (Fig. 1, Fig. 2), and the shape of the graptolite is similar to Western feather pens. Therefore, scientists have named these types of fossils "graptolites" (Bishi). Graptolite fossils are a group of animals that lived in the ancient oceans, called graptolites, and their name was first evolved from the genus Graptolithus, which was created by the Swedish taxonomist Linnaeus in 1735, and means "traces of pens writing in rocks" (Chen Xu et al., 2006; Gong et al., 2020). Graptolites are small filter feeders, with individuals as small as 1-2 mm or less, which live in groups and gather together to build a common exoskeleton. The length of the secreted gracilite bodies can generally reach several centimeters to tens of centimeters, and larger ones can reach 70cm or longer. The largest rhabdosome reported was 1.45 m in length.

Figure 1. Graptolite: (A) Wangjiawan section; (B) and (C graptolite recovery) from the internet

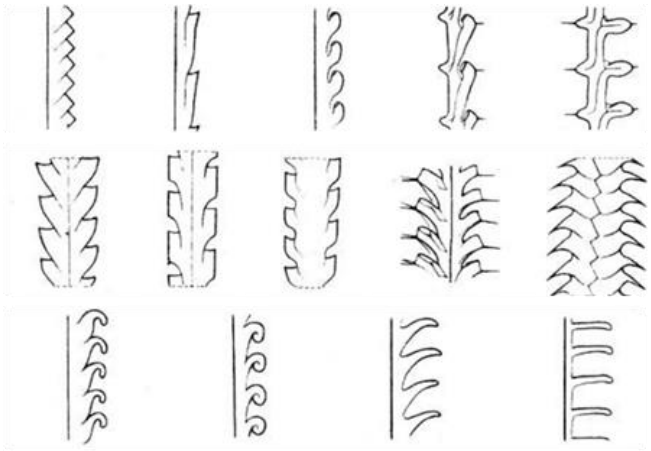

Figure 2. Various forms of fossilized graptolites

Graptolites first appeared in the middle Cambrian of the Paleozoic and lived in groups in marine environments. During the Cambrian period, Graptolite was dominated by benthic arboreal pennofauna, and the evolutionary rate was relatively slow. From the Ordovician onwards, the main body of the graptolites fauna consisted of floating-living orthopelagic pennithischians, and a change in survival strategy led to a rapidly evolving life history from then on. During the Ordovician Great Biological Radiation, the graptolites fauna reached its heyday. Five biological extinction events existed in

geological history. The first biological extinction event occurred at the end of the Ordovician, causing extinction of about 50% of genera and 80% of species of marine animals (Chen et al., 2006). However, numerous fossil evidence suggest that this biological mass extinction did not interrupt the flourishing of graptolite animals, which still flourished widely in the Silurian oceans. In the mid Devonian period, due to the impact of global temperature reduction and sea level decline, graptolites rapidly declined, and most of the orthograptolites became extinct, leaving only a small number of single graptolites and tree graptolites as representatives. At the turn of the Late Devonian to Early Carboniferous, a second biological extinction event occurred on Earth, resulting in the tragic extinction of about 70% of the species of marine fauna (Chen et al., 2006), in which graptolite animals was hard hit. After suffering from events such as lower temperatures, declining sea levels, volcanic eruptions, and severe oxygen deprivation of the Earth, graptolites animal groups died out in large numbers, and eventually became completely extinct in the Carboniferous Period, 200-300 million years ago (Gong et al., 2020). After more than 200 million years, graptolites eventually became extinct. The impact of extinction events on organisms during geologic history is enormous, and the evolution of organisms is irreversible, so I need to protect biodiversity and its ecological environment.

The Uses of Graptolites

What is the role of graptolites? Small graptolites can play an important role in determining the strata age, geological environments and energy resources exploration.

First of all, it is a golden caliper for stratigraphic comparisons and stratigraphic dating. Graptolites are known as the standard fossils in comparative studies of Ordovician, Silurian, and Early Devonian stratigraphy (Gong et al., 2020). During the 4.6 billion years of the Earth's formation, geologists usually use millions of years as the basic unit to distinguish between different periods of geologic history, but the accuracy of inferring stratigraphy from graptolites fossils is much higher than the million-year precision. Paleontologists have found that the evolution of graptolites was very rapid, especially in the Ordovician and Silurian periods, when a large number of new species arose every hundreds of thousands of years, with new evolution occurring at intervals of as little as 100,000 years, thus leaving behind a rich and colorful collection of graptolites fossils. For this reason, graptolites can be used as a golden caliper to determine the stratigraphy age. At present, the international stratigraphic division of the Ordovician and Silurian is mainly based on the graptolites biostratigraphy.

Secondly, the use of graptolites can determine the geological environment at that time. There are two kinds of life style of graptolites: one is fixed on the bottom of the sea, that is, benthic. This type of graptolites animals generally live in shallow water environment, because it is more or less still need some oxygen, the water is too deep cannot survive; another is in the sea water floating life, this part of the graptolites animals can live in more open sea water, can also be in the deep water environment to survive. With the help of these survival characteristics of graptolites animals, paleontologists can speculate and reconstruct the ancient environment where the graptolites are located, such as the depth of seawater, ecological communities and so on. The distribution pattern of graptolites is correlated with the depositional environment, and the transformation of the depositional environment leads to changes in the graptolites basic survival conditions and the preservation conditions. For example, if all the graptolites found in a place are planktonic and not benthic, then it can be inferred that its paleoenvironment was deep water. Nowadays, this identification can be done so finely that five or six depth bands can be delineated based on the type of graptolites fauna, from the surface of the sea water to a depth of a few hundred meters, with a specific assemblage of graptolites fauna in each depth band.

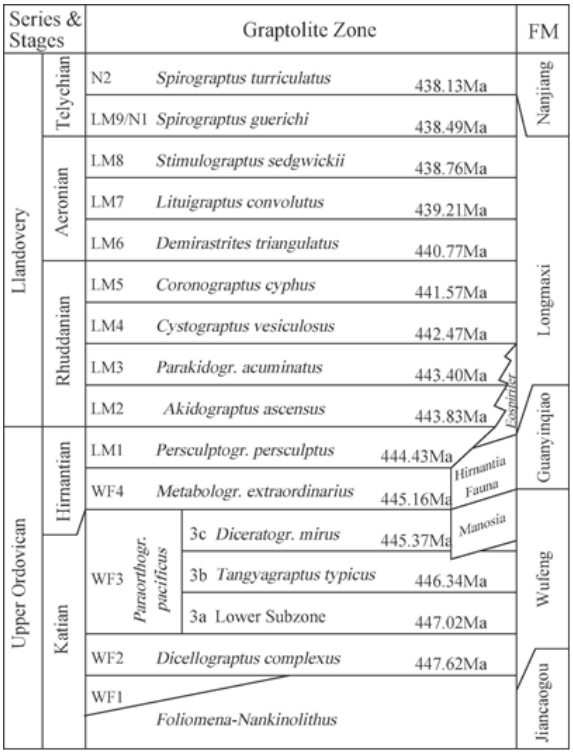

Figure 3. Scheme for delineation of graptolite zones in Wufeng Formation (WF), Longmaxi Formation (LM) and Nanjiang Formation (N) in the Yangtze block (Chen Xu et al., 2015, 2017)

Third, it can be used to guide the shale gas exploration and development. Shale gas is mainly produced in the Ordovician to Silurian strata in China, and the Ordovician to Silurian black shale contains a large number of graptolites. The graptolites shale section of the bottom of Wufeng - Longmaxi Formation is a shale gas-rich section, which contains a lot of graptolites fossils. The graptolites calibration can provide a key basis for searching for high-quality shale reservoir segments and clarifying the best target location and objectives, thus better guiding shale gas exploration and development. Based on the basic principles and methods of graptolites biostratigraphy, Chen Xu et al.(2015, 2017, 2018) established a graptolites bibelot delineation scheme for the Wufeng Formation (WF), Longmaxi Formation (LM), and Nanjiang Formation (N) through extensive comparative analysis of the iconic graptolites fossils in the Yangtze block (Figure 3), and proposed that WF2 to WF3 of the Wufeng Formation and LM1 to LM5/LM6 of the Longmaxi Formation are the main hydrocarbon source rock layers and reservoirs for shale gas production. This scheme has been used as a "time scale" for fine stratigraphic delineation and regional comparison of the Wufeng Formation and Longmaxi Formation in drilling wells and outcrop areas, which is an important guide to the selection of favorable shale gas layers and favorable zones (Figure 4, Gong et al., 2020).

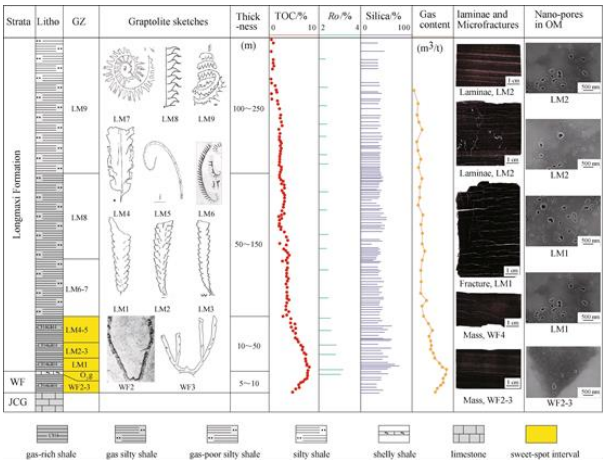

Figure 4. Graptolite biostratigraphy and reservoir characteristics of the Wufeng-Longmaxi Shale in South China. The sweet-spot interval for shale gas exploration corresponds to graptolite zones WF2-LM5. Litho = lithology; GZ = graptolite zone; WF = Wufeng Formation; JCG = Jiancaogou Formation (Gong et al., 2020).

Geological setting of the Wangjiawan section

The Wangjiawan section is located in Wangjiawan Village, Fenxiang Town, 42 km northern of Yichang City, Hubei Province, China (Fig. 5), with latitude and longitude of N 30°58′28.66″, E 111°25′24.80″. It is the global standard stratigraphic section and point (GSSP) of the Ordovician Hernantian Stage "Golden Spike" (445.2 ± 1.4 Ma).

“Hernantian stage” is the seventh order of the Ordovician, that is, the top of a "golden spike", although its time limit is short, only 1.8 million years, but the establishment of the "Hernantian stage" has an important significance. The establishment of the "Hernantian stage" is of great significance. It records the second largest biological extinction (85% of species extinctions) since the Phanerozoic, the expansion of the Antarctic Ice Sheet leading to climate cooling, and the global sea level drop (Chen et al., 2006; Sheehan, 2001), which provides a unified time standard for the precise comparison of global stratigraphy and for the study of global biological and environmental events.

The Wufeng Formation and Longmaxi Formation are exposed in the northern section of Wangjiawan Village. The Wufeng Formation mainly consists of dark grey and grey-black thinly bedded siliciclastic rocks and siliciclastic shale rhyolitic interbedded with a lot of graptolites. The top Wufeng Formation is Guanyinqiao section, which is greyish-yellow medium-layered tuffs, tuffaceous mudstones, and powdery-fine sandstone, with a large number of brachiopod and other mesocoelous fossils and trilobite fossils, which is only 20 cm thick in the Wangjiawan section. The Longmaxi Formation is a thin layer of silica-bearing carbonaceous mudstone, with a thickness of more than 2 meters; at the bottom is a gray-black carbonaceous shale, with a thickness of about 50 meters in this region. Only the Longmaxi Formation bottom is exposed in the Wangjiawan section, which contains a lot of graptolites fossils

(Fig. 3, Fig. 6). The "Hernantian stage" gold spike section is established 0.39 m below the bottom boundary of the Guanyinqiao Formation (Chen Xu et al. 2006), consistent with first occurrence of Normal graptolites extraordinarius.

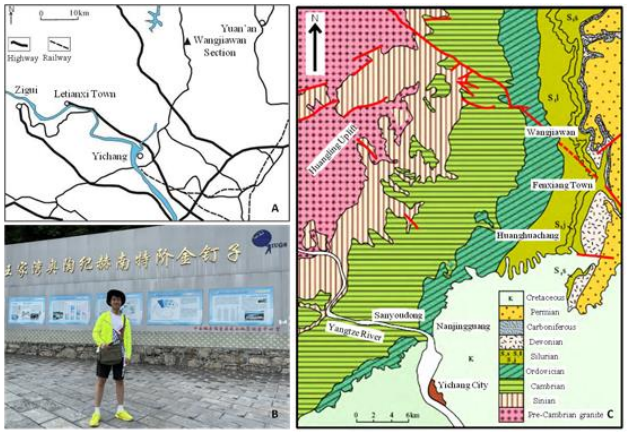

Figure 5 Location of Wangjiawan profile: (A) transportation location map;

(B) photographs of field work; (C) geologic sketch map

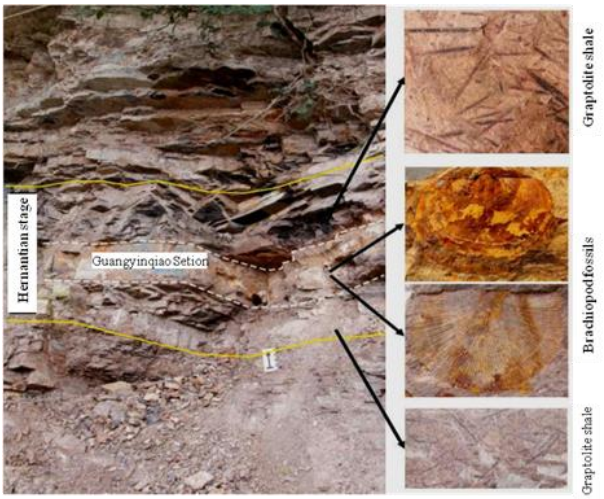

Figure 6. Stratigraphic distribution and biofossils in the Wangjiawan section

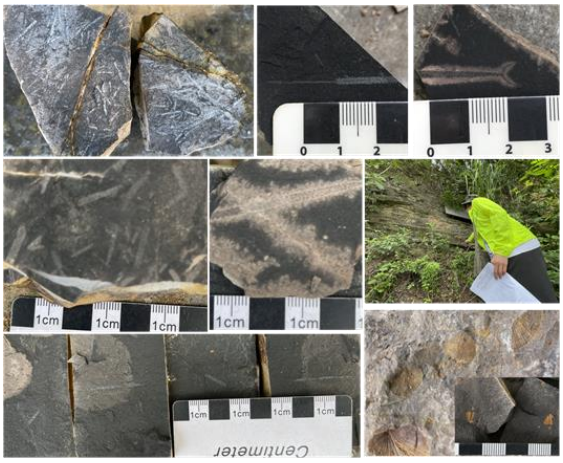

Figure 7. Graptolites, Hernanterbe and trilobites Fossils samples collected from the Wangjiawan section in Three Gorges.

Methodology and Investigation

On July 21, 2023, I traveled to the Wangjiawan section to conduct field investigation, on-site profile measurement and sample collection (Figs. 5, 7). 16 samples of various graptolite fossils, 5 Longmaxi Formation black shale samples, 2 Hernanterbe fossil samples, and 2 trilobite fossil samples were collected.

At present, organic matter maturity studies mainly use Raman spectroscopy, vitrinite reflectance and microfluorescence techniques. The reflectance of solid bitumen, Raman spectroscopy, and random reflectance of graptolite body on the collected samples will analyzed for the organic matter maturity of the Wangjiawan section in the Three Gorges area. These methods are briefly described in the following texts.

Solid Bitumen Reflectance Method

The vitrinite reflectance is the most reliable organic matter maturity parameter of hydrocarbon source rocks since the Late Paleozoic. The main sources of sedimentary organic matter in the Lower Paleozoic marine source rocks are algae and bacteria, followed by bioclastic organic fractions. Solid bitumen is the most important secondary microcomponent after the source rock maturity stage. In the marine hydrocarbon source rock that lacks vitrinite of higher plant origin, solid bitumen reflectance is

usually used to convert to equivalent vitrinite reflectance for the evaluation of the source rock maturity.

Solid bitumen, as secondary organic matter, is a product of the subsequent transport of oil generated and excreted by casein, filling the pores and fractures, angular and bounded by carbonate minerals. The factors controlling the origin of solid bitumen depend primarily on type and content of organic microcomponent precursors and, to a lesser extent, on the geological factors controlling its generation (temperature, pressure, microbial activity) and destruction (cracking, deasphalting, biodegradation). Due to the diversity of bitumen genesis and the complexity of its characteristics, the identification and recognition of microscopic components is the key to the determination of bitumen reflectance. In the kerogen optical section, solid bitumen shares many similar reflective characteristics with other vitrinite components, but their shape, structure, and orientation differ in whole rock optical section. Correctly distinguishing the characteristics of solid bitumen is a prerequisite for measurement bitumen reflectance.

Raman Spectroscopy Method

Raman spectroscopy is a technique based on Raman scattering phenomenon, which can directly obtain the molecular vibration information of each material group in the sample. Raman spectrum has rich and sharp characteristic peaks, based on the number; position and intensity of the peaks can be qualitatively and quantitatively analyzed for the test samples when the experimental conditions such as incident light frequency and intensity are determined.

Raman spectroscopy is a type of scattering spectroscopy. By characterizing the parameters of the first order vibration peaks of solid carbonaceous materials Raman spectra in sedimentary/metamorphic rocks, it can be used to study molecular structure of carbonaceous materials and paleogeological temperatures/maturity. Raman spectroscopy can play an important role in the field of fluid inclusions, sedimentary organic matter, rock and mineral identification, because of the advantages of simple sample preparation, convenient and fast testing and short cycle time.

4.3 Graptolite Epidermis Reflectance Method

Graptolites' epidermal bodies are characterized by two morphologies: non-granular and granular. The non-granular graptolites are usually distributed in strips and bands along the layers, and are often segmented and interrupted; they have smooth surfaces, high reflectivity, and obvious anisotropy; some of them have residual biological structures such as body walls and cell tubes,which are often filled with strawberry shaped pyrite. It is easy to observe the spindle layered biological layer structure on parallel bedding planes with good polishing effect, and the higher the maturity, the more obvious this phenomenon becomes. The surface of granular graptolites is mostly elliptical in shape, with a long axis direction usually consistent with the bedding direction. The surface is rough, with a clear graininess, low reflectivity, and weak anisotropy.

Implications and Discussions

Graptolite reflectance and equivalent vitrinite reflectance

The shale organic matter is mainly composed of solid bitumen and graptolite fragments, with a small amount of vitrinite and chitin (Figure 8). The shale samples were ground into rock chips small enough to pass through a 20-mesh sieve. These chips were then formed into whole-rock pellets using procedures typical of standard coal petrography. The petrographic features of the macerals were documented using a Leica DM2700 P microscope, employing a 50× oil immersion objective and observed under either white or blue light. Semi-quantitative maceral composition was determined based on visual estimate at an increment of 5%. Vitrinite reflectance (Ro) was measured using the Leica DM2700 P microscope and the computer program DISKUS-FOSSIL from Hilgers Technisches Buero. Reflectance standards yttrium-aluminum-garnet (YAG) (reflectance

0.891%) and gadolinium-gallium-garnet (GGG) (reflectance 1.713%) were used for reflectance calibration.

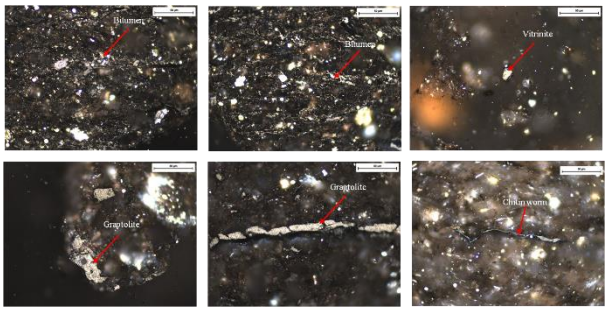

Figure 8. Microscopic photographs of shale organic matter composition.

The main focus is on reflectance testing for solid bitumen and graptolite fragments. The graptolite reflectance (GRo) is generally converted into equivalent vitrinite reflectance (EqRo) using the formula EqRo = 0.99×GRo+0.08 (Luo et al., 2020). For bitumen reflectance (BRo), it is typically converted into EqRo using the formula EqRo = 0.6569×BRo +0.3364 (according to Feng Guoxiu et al., 1988). The relationship between rock pyrolysis temperature Tmax and EqRo is converted using the formula EqRo = 0.018 ×Tmax-7.16 (Jarvie et al., 2001). In this experiment, the reflectance of solid bitumen for 3 samples and the reflectance of graptolites for 3 samples were measured (Figure 9), and the results are shown in Table 1. From the results, the EqRo converted from solid bitumen reflectance indicates a lower shale maturity (1.098-1.110%), while the shale maturity revealed by graptolite reflectance is relatively higher (1.245-1.253%).

Table 1. The reflectance (Ref.) experiments results

Sample No.	Objects	Number	Ref. Max	Ref. Min	Mean	S.D.	EqRo	Tmax (℃)
LMX1	bitumen	165	1.579	0.709	1.178	0.217	1.110	459.44
LMX2	bitumen	101	1.669	0.684	1.159	0.251	1.098	458.78
LMX3	bitumen	121	1.659	0.718	1.171	0.225	1.105	459.20
BS1	graptolite	85	1.606	0.842	1.185	0.171	1.253	467.39
BS2	graptolite	106	1.684	0.796	1.177	0.152	1.245	466.94
BS3	graptolite	122	1.619	0.765	1.178	0.161	1.246	467.00

EqRo = 0.99×GRo+0.08 (Luo et al., 2020)；EqRo = 0.6569×BRo +0.3364（Feng Guoxiu et al.，1988）；EqRo = 0.018 ×Tmax-7.16 (Jarvie et al., 2001)

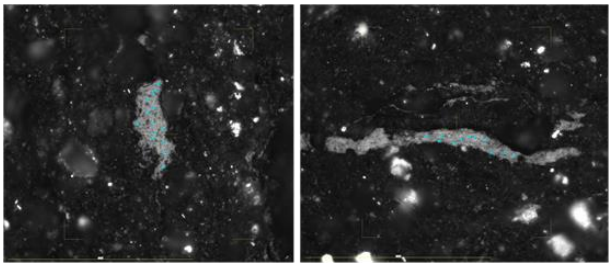

Figure 9. Microscopic photographs of shale graptolite reflectance measurement points.

Raman spectroscopy and equivalent vitrinite reflectance

The morphologies of the laser Raman analysis spectra of various types of solid organic matter, along with the displacement and peak height ratio parameters of the D and G peaks, fully reflect various pieces of information such as molecular vibrations of carbonaceous material during thermal evolution, and can be used as a basis for evaluating the thermal evolution degree of samples or the temperature conditions of experimental samples. Liu Dehan et al. (2013), Wilkins et al. (2014, 2015), Baludikay et al. (2018) established two quantitative characterization formulas of solid organic matter Raman spectroscopy parameters with thermal evolution degree at different organic matter maturity stages. Among them, the model calculation formula established by the relationship between peak interval *d*(G-D) and vitrinite reflectance from mature to highly mature stage is as follows:

$$Rmc\ \text{Ro\%} = 0.0537 \times d(\text{G-D}) - 11.21$$

Where *Rmc*Ro% is the reflectance calculated by Raman analysis parameters, *d*(G-D) is the peak interval of Raman displacement. The calculation formula for calculating the maximum burial temperature from *Rmc*Ro% is as follows:

$$Tpeak\ burial\ (°C) = (\ln(Rmc\text{Ro\%}) + 1.68)/0.0124$$

For over-mature samples, regression of the peak height ratio parameters (Dh/Gh) in Raman spectroscopy analysis with vitrinite reflectance data (Figure 4) yields the match relationship between the peak height ratio and vitrinite reflectance.

$$Rmc\text{Ro\%} = 1.1659 \times h(\text{Dh/Gh}) + 2.7588$$

Where *Rmc*Ro% is the reflectance calculated by Raman analysis parameters, *h*(Dh/Gh) is the peak height ratio (Dh is the height of the D peak, Gh is the height of the G peak). The calculation formula for calculating the maximum burial temperature from *Rmc*Ro% is as follows:

$$Tpeak\ burial\ (°C) = (\ln(Rmc\text{Ro\%}) + 1.19)/0.00782$$

In this experiment, Raman spectroscopy of the organic matter in three shale samples was measured (Figure 10), with the spectral peaks being the D peak and G peak. The peak intensity results are shown in Table 2. For sample BS1, six measurement points yielded Raman reflectance values calculated based on the peak interval of D and G peaks Raman shifts, ranging from 0.626554 to 0.894517%, with an average of 0.7415%, and the corresponding temperatures calculated were between 97.78°C and 126.49°C. For sample BS2, eight measurement points resulted in Raman reflectance values from 0.790339 to 1.106095%, with an average of 0.9057%, and the calculated temperatures were between 116.51°C and 143.62°C. For sample BS3, four measurement points yielded Raman reflectance values from 0.932107 to 1.009453%, with an average of 0.9663%, and the temperatures calculated were between 129.81°C and 136.24°C. Compared to the equivalent vitrinite reflectance converted from solid bitumen reflectance (1.098-1.110%) and the shale maturity indicated by graptolite reflectance (1.245-1.253%), the organic matter maturity (Raman *Rmc*Ro%) obtained from the organic matter Raman spectroscopy of the shale samples in this experiment is lower, averaging 0.7415~0.9663%. Lower maturity samples may have fluorescence interference causing the experimental data to be more dispersed (Quirico, 2005; Henry, 2018).

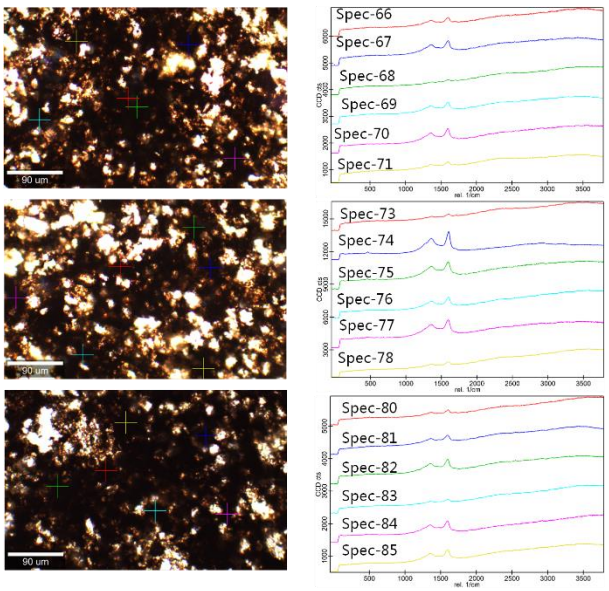

Figure 10. Raman spectroscopy results of shale organic matter
(spectral peaks are D peak and G peak).

Regionally, the organic matter maturity of the Wufeng-Longmaxi shale previously tested in the Yichang Three Gorges area generally exceeds 1.4%. For instance, the organic matter maturity of the Wufeng-Longmaxi shale in Badong Jianyangping was tested to be 1.4%, and in Yichang Zhicheng, it was 1.9%. In the Sichuan Basin and its periphery areas, the organic matter maturity of the Wufeng-Longmaxi shale generally ranges from 2.0 to 4.0% (Xie Xinong et al., 2019), reaching the over-mature stage. The results of this test are generally low, which is speculated to be related to the Early Silurian "Yichang Uplift" (Chen Xu et al., 2018). Due to the uplift and the missing strata, the burial is shallow; the paleo-temperature is not high, resulting in lower maturity.

Table 2. The Laser Raman spectroscopy experiments results of shale organic matter

Sample No.	Name	D4-band			D1-band			D3-band			G-band			D2-band			R_{mc}/%	In (R_{mc}/%)	$T_{peak\ heat}$ (°C)	Mean R_{mc}/%
		Position	width	Area	Position	width	Area	Position	width	Area	Position	width	Area	Position	width	Area				
B51-T	Spec-60	1281.8	203.62	9156.4	1360.9	92.545	5744.4	1470.1	325.89	11750	1584.46	63.179	4488.6	1606.5	37.131	3092.5	0.794635	-0.22987239	116.945775	0.7451
B51-T	Spec-67	1289.9	225.44	30385	1365.2	97.516	15851	1468.4	109.21	7382.9	1586.13	85.265	19755	1605.8	35.908	4882.6	0.652867	-0.42638185	101.098238	
B51-T	Spec-69	1299.4	229.39	42103	1364.9	85.732	15417	1465.6	89.494	7207	1585.51	85.393	22604	1604.9	37.671	7273.8	0.638368	-0.44884036	99.2870678	
B51-T	Spec-70	1288.3	221.99	22037	1358.4	87.036	9529.7	1474.1	331.07	26412	1578.82	59.286	7346.4	1603.7	40.43	6983.2	0.626554	-0.46752032	97.7806197	
B51-T	Spec-74	1272.7	180.45	67617	1359.4	101.81	58547	1465.7	239.41	52858	1584.27	59.486	34410	1606.7	38.371	30137	0.863908	-0.146289	123.686371	
B51-T	Spec-77	1249.1	232.75	18817	1355.7	134.82	22394	1474.8	120.23	6843	1581.11	84.996	14926	1602.9	41.155	4992.9	0.894517	-0.11147137	126.494244	
B52-T	Spec-6	1278.8	199.43	39010	1356.7	94.201	22419	1463.4	336.8	50510	1580.2	51.448	12731	1604.2	39.531	18005	0.790339	-0.23529331	116.936604	0.9057
B52-T	Spec-7	1273	212.68	23217	1354.8	98.894	14832	1466	332.96	30117	1580.53	55.524	7798.9	1603.9	40.861	10602	0.909553	-0.09480201	127.838548	
B52-T	Spec-13	1286	229.25	49142	1358	89.012	21678	1459	290.89	39801	1581.66	53.724	15149	1605.8	39.126	17639	0.80269	-0.21978669	117.759138	
B52-T	Spec-14	1284.6	229.15	47717	1356.6	93.532	19913	1476.5	296.6	39118	1580.1	56.344	14882	1603.7	38.974	14835	0.794635	-0.22987239	116.945775	
B52-T	Spec-15	1278.5	284.31	36035	1354.7	121.14	18920	1472.6	150.63	9845.3	1578.67	83.672	17140	1600.5	44.328	6753.1	0.8188	-0.19991543	119.361659	
B52-T	Spec-18	1277.6	201.38	41226	1356.8	97.211	23137	1471.5	333.47	50619	1583.18	55.484	16941	1605	37.764	15010	0.944995	-0.05657564	130.921319	
B52-T	Spec-19	1271.6	176.25	30846	1359.5	101.38	29071	1466.8	159.85	16275	1588.34	64.151	22477	1607.4	35.398	10942	1.078171	0.07526689	141.553717	
B52-T	Spec-27	1267.6	167.21	39065	1357.8	109.9	46706	1469.9	164.86	22550	1587.13	66.161	28634	1607	36.135	17521	1.106595	0.10083579	143.61379	
B53-T	Spec-32	1283.3	219.34	36513	1357.9	91.028	15665	1472.9	288.96	28770	1585.48	56.91	13402	1605.9	36.228	10471	1.009435	0.08939077	136.241191	0.9663
B53-T	Spec-38	1295.7	248.7	36725	1361.1	93.028	12806	1470.1	116.94	6326.5	1587.17	70.094	14175	1605.5	36.475	7567.1	0.932107	-0.07030766	129.813098	
B53-T	Spec-44	1264.5	191.15	26140	1357.8	111.28	25504	1469.4	132.11	10671	1584.55	71.077	18252	1605.1	37.497	9278.5	0.966475	-0.03489985	132.733883	
B53-T	Spec-45	1280.5	244.1	30611	1357.7	102.62	14280	1471.4	147.05	8726.8	1584.26	72.267	14007	1602.9	38.485	6330.8	0.957346	-0.04359841	131.968516	

The correlation of reflectance calculated by three methods

The correlation regression of equivalent vitrinite reflectance data obtained by three methods was performed (Figure 11). As shown in Figure 11, the correlation between solid bitumen reflectance and graptolite epidermis reflectance is 0.7663, between solid bitumen reflectance and Raman spectroscopy reflectance is 0.9748, and between graptolite epidermis reflectance and Raman spectroscopy reflectance is 0.6203. The best correlation is observed between solid bitumen reflectance and Raman spectroscopy reflectance, followed by the correlation between solid bitumen reflectance and graptolite epidermis reflectance, with the weakest being the correlation between graptolite epidermis reflectance and Raman spectroscopy reflectance. However, overall, all correlations are greater than 0.6, which indicates that they can be used to characterize the maturity of organic matter.

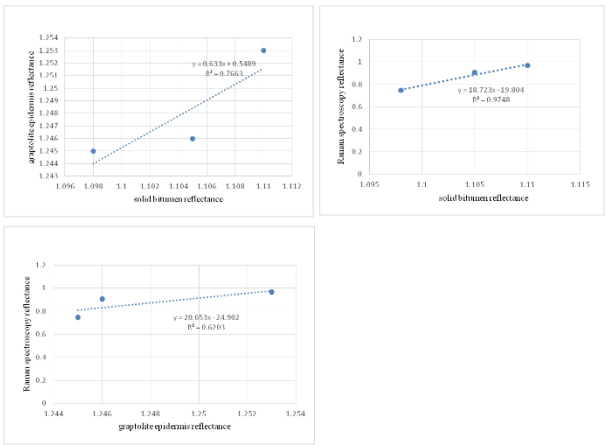

Figure 11. The correlation regression of equivalent vitrinite reflectance data obtained by three methods

As shown in Figure 11, the relationship between Raman reflectance and graptolite reflectance is expressed as:

$$R_{mc}\text{Ro\%} = 20.653\text{GRo} - 24.902$$

The formula previously mentioned for calculating the maximum burial temperature from *Rmc*Ro% is:

Tpeak burial (°C) = (ln (*Rmc*Ro%) + 1.68)/0.0124

From these two formulas, the calculation formula for the relationship between graptolite reflectance and maximum burial temperature is derived as:

Tpeak burial (°C) = (ln (20.653GRo – 24.902) + 1.68)/0.0124

Where *Rmc*Ro% is the reflectance calculated by Raman analysis parameters, *GRo* is the graptolite epidermis reflectance, and *Tpeak burial* (°C) is the maximum burial paleotemperature.

Therefore, based on the analysis in this study, a relationship between graptolite reflectance and paleotemperature has been established. Graptolite reflectance can serve as a temperature indicator for the maturity of shale organic matter, and it is the best and relatively more accurate indicator compared to solid bitumen reflectance and Raman spectroscopy reflectance.

Conclusion

（1）The Wufeng-Longmaxi Formation of Wangjiawan section in the Three Gorges is the global standard stratigraphic section and point (GSSP) for the Ordovician Hernantian Stage. The top Wufeng Formation is the Guanyinqiao Member, characterized by greyish-yellow medium-bedded tuffaceous mudstone and fine to very fine sandstone, containing abundant brachiopod and trilobite fossils. The Longmaxi Formation is composed of greyish-black thin-layered siliceous carbonaceous mudstone and carbonaceous shale, rich in graptolite fossils.

（2）The organic matter maturity was calculated using three methods. The equivalent vitrinite reflectance converted from solid bitumen reflectance is 1.098-1.110%, the shale maturity revealed by graptolite reflectance is 1.245-1.253%, and the average organic matter maturity obtained from calculations based on organic matter Raman spectroscopy is 0.7415~0.9663%.

（3）The correlation regression was performed on the equivalent vitrinite reflectance data obtained by three methods. The correlation between solid bitumen reflectance and graptolite epidermis reflectance was 0.7663, between solid bitumen reflectance and Raman spectroscopy reflectance is 0.9748, and between graptolite epidermis reflectance and Raman spectroscopy reflectance is 0.6203. All are greater than 0.6, and these three methods can be used to characterize the organic matter maturity. The study established the relationship between the graptolite epidermis reflectance and paleotemperature.

Conflict of Interests: the author has claimed that no conflict of interests exists.

References

1. Bertrand, R., 1990. Correlations among the reflectances of vitrinite, chitinozoans, graptolites and scolecodonts. Org. Geochem. 15, 565–574.
2. Bertrand, R., 1993. Standardization of solid bitumen reflectance to vitrinite in some Paleozoic sequences of Canada. Energy Sources 15, 269–287.
3. Chen, X., Rong, J.Y., Charles, E.M., David, A.T.H., Fan, J.X., Zhan, R.B., Zhang, Y.D., Li, R.Y., Wang, Y., 2000. Late Ordovician to earliest Silurian graptolite and brachiopod biozonation from the Yangtze region, South China, with a global correlation. Geol. Mag. 137, 623–650.
4. Chen, X., Fan, J., Wang, W., Wang, H., Nie, H., Shi, X., Wen, Z., Chen, D., Li, W., 2017. Stage-progressive distribution pattern of the Lungmachi black graptolitic shales from Guizhou to Chongqing, Central China. Sci. China Earth Sci. 60, 1133–1146.
5. Chen, X., Fan, J., Zhang, Y., Wang, H., Chen, Q., Wang, W., Liang, F., Guo, W., Zhao, Q., Nie, H., Wen, Z., Sun, Z., 2015. Subdivision and delineation of the Wufeng and Lungmachi black shales in the subsurface areas of the Yangtze platform. J.

Stratigr. 39, 351–358 (in Chinese with English abstract).
6. Chen X., Rong J., Fan J., Zhan R., Mitchell C.E., Harper D. 2006. The global boundary stratotype section and point (GSSP) for the base of the Hirnantian Stage (the uppermost of the Ordovician System). Episodes, 29: 183–196.
7. Chen, X., Rong, J., Charles, M., David, H., Fan, J., Zhan, R., Zhang, Y., Li, R., Wang, Y., 2000. Late Ordovician to earliest Silurian graptolite and brachiopod biozonation from the Yangtze region, South China, with a global correlation. Geol. Mag. 137, 623–650.
8. Chen, X., Rong, J., Li, Y., Boucot, A., 2004. Facies patterns and geography of the Yangtze region, South China, through the Ordovician and Silurian transition. Palaeogeogr. Palaeoclimatol. Palaeoecol. 204, 353–372.
9. Chen, X., Rong, J., Michael, M., David, S., Charles, M., Fan, J., 2005. Patterns and processes of latest Ordovician graptolite extinction and recovery based on data from South China. J. Paleontol. 79, 824–861.
10. Chen X, Chen Q, Zhen Y Y, Wang H Y, Zhang L N, Zhang J P, Wang W H, Xiao Z H. 2018. Circumjacent distribution pattern of the Lungmachian graptolitic black shale (early Silurian) on the Yichang Uplift and its peripheral region. Science China Earth Sciences, 61: 1195–120.
11. Gong Jianming, Qiu Zhen, Zou Caineng, Wang Hongyan, Shi Zhensheng. 2020. An integrated assessment system for shale gas resources associated with graptolites and its application. Applied Energy, 262: 114524.
12. Guedes, A., Valentim, B., Prieto, A.C., Rodrigues, S., Noronha, F., 2010. Micro-Raman spectroscopy of collotelinite, fusinite and macrinite. Int. J. Coal Geol. 83, 415–422.
13. Guo, T.L., Zhang, H.R., 2014. Formation and enrichment mode of Jiaoshiba shale gas field, Sichuan Basin. Petrol. Explor. Dev. 41, 31–40 (in Chinese with English abstract).
14. Hackley, P.C., Cardott, B.J., 2016. Application of organic petrography in North American shale petroleum systems: a review. Int. J. Coal Geol. 163, 8–51.
15. Hao, F., Zou, H., Lu, Y., 2013. Mechanisms of shale gas storage: implications for shale gas exploration in China. AAPG Bull. 97, 1325–1346.
16. Henry, D.G., Jarvis, I., Gillmore, G., Stephenson, M., Emmings, J.F., 2018. Assessing lowmaturity organic matter in shales using Raman spectroscopy: Effects of sample preparation and operating procedure. Int. J. Coal Geol. 191, 135–151.
17. Jacob, H., 1989. Classification, structure, genesis and practical importance of natural solid oil bitumen ("migrabitumen"). Int. J. Coal Geol. 11, 65–79.
18. Jarvie, D.M., Hill, R.J., Ruble, T.E., Pollastro, R.M., 2007. Unconventional shale-gas systems: the Mississippian Barnett Shale of north-central Texas as one model for thermogenic shale-gas assessment. Bull. 91, 475–499.
19. Jin Zhijun, Hu Zongquan, Gao Bo. 2016. Controlling factors on the enrichment and high productivity of shale gas in the Wufeng-Longmaxi Formations , southeastern Sichuan Basin. Earth Science Frontiers, 23(1): 1-10.
20. Liu, D.H., Xiao, X.M., Tian, H., Min, Y.S., Zhou, Q., Cheng, P., Shen, J.G., 2013. Sample maturation calculated using Raman spectroscopic parameters for solid organics: methodology and geological applications. Chin. Sci. Bull. 58, 1285–1298.
21. Luo, Q.Y., Fariborz G., Zhong N.N., Wang Y., Qiu N.S., Skovsted C.B., Niels H.S., Schovsbo V.S., Morga R., Xu Y., Hao J., Liu A., Wu J., Cao W.n, Min X., Wu J. 2020. Graptolites as fossil geo-thermometers and source material of hydrocarbons: An overview of four decades of progress. Earth-Science Reviews, 200: 103000.
22. Luo, Q., Hao, J., Skovsted, C.B., Luo, P., Khan, I., Wu, J., Zhong, N., 2017. The organic petrology of graptolites and maturity assessment of the Wufeng–longmaxi Formations from Chongqing, China: insights from reflectance cross-plot analysis. Int. J. Coal Geol. 183, 161–173.

23. Luo, Q., Hao, J., Skovsted, C.B., Xu, Y., Liu, Y., Wu, J., Zhang, S., Wang, W., 2018. Optical characteristics of graptolite-bearing sediments and its implication for thermal maturity assessment. Int. J. Coal Geol. 195, 386–401.
24. Luo, Q., Hao, J., Li, K., Xu, Y., Wang, X., Wang, H., Luan, J., Hu, K., Li, T., Zhong, N.,2019. A new parameter for the thermal maturity assessment in the palaeozoic sediments: a restudy on the optical characteristics of the graptolite. Acta Geol. Sin. (Chin. Ed.) 93 (9), 2362–2371 (in Chinese with English abstract).
25. Mastalerz, M., Schimmelmann, A., Drobniak, A., Chen, Y., 2013. Porosity of Devonian and Mississippian New Albany Shale across a maturation gradient: insights from organic petrology, gas adsorption, and mercury intrusion. AAPG Bull. 97, 1621–1643.
26. Meng Jianghui, Lyu Peixi, Wu Wei, Pan Renfang, Zhu Yiqing. 2022. A method for evaluating the thermal maturity of marine shale based on graptolite reflectance and Raman spectroscopy: A case from the Lower Palaeozoic Wufeng–Longmaxi Formations, southern Sichuan Basin, SW China. Oil and Gas Geology, 43(6):1515-1528 (in Chinese with English abstract).
27. Petersen, H.I., Schovsbo, N.H., Nielsen, A.T., 2013. Reflectance measurements of zooclasts and solid bitumen in lower Palaeozoic shales, southern Scandinavia: correlation to vitrinite reflectance. Int. J. Coal Geol. 114, 1–18.
28. Qiu, Z., Zou, C., Li, X., Wang, H., Dong, D., Lu, B., Zhou, S., Shi, Z., Feng, Z., Zhang, M., 2018. Discussion on the contribution of graptolite to organic enrichment and gas shale reservoir: a case study of the Wufeng–longmaxi shales in South China. J. Nat. Gas Geosci. 3, 147–156.
29. Quirico, E., Rouzaud, J.N., Bonal, L., Montagnac, G., 2005. Maturation grade of coals as revealed by Raman spectroscopy: progress and problems. Spectrochim. Acta Part A Molecular and Biomolecular Spectroscopy 61, 2368–2377.
30. Tissot, B.P., Welte, D.H., 1984. Petroleum Formation and Occurrence. Seconded. Springer-Verlag, Berlin, pp. 699.
31. Wang, M., Li, Z.S., 2016. Thermal maturity evaluation of sedimentary organic matter using laster Ramman spectroscopy. Acta Pet. Sin. 37, 1129–1136 (in Chinese with English abstract).
32. Wang, Y., Qiu, N.S., Tenger, B., Shen, B.J., Xie, X.M., Ma, Z.L., Lu, C.J., Yang, Y.F., Yang, L., Cheng, L.J., Fang, G.J., Cui, Y.. 2019. Integrated assessment of thermal maturity of the Upper Ordovician–Lower Silurian Wufeng–Longmaxi shale in Sichuan Basin, China. Marine and Petroleum Geology,100: 447-465.
33. Wang Y, Qiu N, Xie X, Ma Z.L., Lu C.J. 2021. Maturity and thermal evolution differences between two sets of Lower Palaeozoic shales and its significance for shale gas formation in south-western Sichuan Basin, China. Geological Journal, 56(7): 3698-3791.
34. Wei, G., Chen, G., Du, S., Zhang, L., Yang, W., 2008. Petroleum systems of the oldest gas field in China: Neoproterozoic gas pools in the Weiyuan gas field, Sichuan Basin. Mar. Petrol. Geol. Wilkins, R.W.T., Boudou, R., Sherw
35. Wilkins, R.W.T., Boudou, R., Sherwood, N., Xiao, X., 2014. Thermal maturity evaluation from inertinites by Raman spectroscopy: the ‘RaMM’ technique. Int. J. Coal Geol. 128–129, 143–152.
36. Wilkins, R.W.T., Wang, M., Gan, H., Li, Z., 2015. A RaMM study of thermal maturity of dispersed organic matter in marine source rocks. Int. J. Coal Geol. 150–151, 252–264.
37. Yang Yunfeng. 2016. Application of bitumen and graptolite reflectance in the Silurian Longmaxi shale， southeastern Sichuan Basin. Petroleum Geology and Experiment, 38(4): 466-472 (in Chinese with English abstract).
38. Zhang, T.W., Ellis, G.S., Ruppel, S.C., Milliken, K., Yang, R.S., 2012. Effect of organic matter type and thermal maturity on methane adsorption in shale-gas systems. Org. Geochem. 47, 120–131.

39. Zhou Q. Xiao X, Pan L. 204.The relationship between micro-Raman spectral parameters and reflectance of solid bitumen. International Journal of Coal Geology, 121: 19-25.
40. Zou, C.N., Yang, Z., Dai, J.X., Dong, D.Z., Zhang, B.M., Wang, Y.M., Deng, S.H., Huang, J.L., Liu, K.Y., Yang, C., Wei, G.Q., Pan, S.Q., 2015. The characteristics and significance of conventional and unconventional Sinian–Silurian gas systems in the Sichuan Basin, central China. Mar. Petrol. Geol. 64, 386–440.
41. Zou, C., Dong, D., Yang, H., Wang, Y., Huang, J., Wang, S., Fu, C., 2011. Conditions of shale gas accumulation and exploration practices in China. Nat. Gas Ind. 31, 26–39 (in Chinese with English abstract).